

# Chemical Science

Volume 12  
Number 4  
28 January 2021  
Pages 1179–1570

rsc.li/chemical-science



ISSN 2041-6539

**EDGE ARTICLE**

Yulan Chen *et al.*

Empowering self-reporting polymer blends with orthogonal optical properties responsive in a broader force range

Cite this: *Chem. Sci.*, 2021, 12, 1245

All publication charges for this article have been paid for by the Royal Society of Chemistry

# Empowering self-reporting polymer blends with orthogonal optical properties responsive in a broader force range†

Mengjiao Wu, Zhen Guo, Weiye He, Wei Yuan and Yulan Chen \*

Self-reporting polymers, which can indicate damage with perceptible optical signals in a tailored force range, are useful as stress-sensitive sensors. We demonstrate a simple approach to realize this function by embedding two distinct mechanophores – rhodamine (**Rh**) and bis(adamantyl)-1,2-dioxetane (**Ad**), in polyurethane/poly(lactic acid) blends. The deformed blends generate red coloration and red chemiluminescence. Such a unique dual-responsive behavior was evaluated by solid-state UV-vis spectroscopy, macroscopic tensile tests with *in situ* RGB and light intensity analyses, which supported a stress-correlated occurrence of the ring-opening of **Rh**, the scission of **Ad** and the fluorescence resonance energy transfer process between the respective mechanochemical species. Complementarity stemming from the difference in properties and manifestations of the two mechanophores is essential. That is, the more labile **Rh** allows shifting the appreciable optical changes to a much lower force threshold; the transient nature and high dynamic range of mechanochemiluminescence from **Ad** map in real time where and when many of the covalently incorporated dioxetane bonds break; besides, the disrupted yet non-scissile structure of **Rh** acts as a fluorescent acceptor to effectively harvest chemiluminescence from ruptured **Ad**. The current strategy is thus empowering multi-functional mechano-responsive polymers with greatly improved sensitivity and resolution for multimodal stress reporting.

Received 8th November 2020  
Accepted 24th November 2020

DOI: 10.1039/d0sc06140a

rsc.li/chemical-science

## Introduction

Stress induced covalent bond scission underlies the macroscopic failure of polymeric materials.<sup>1</sup> The possibility to monitor mechanical stress and deformation at broader time and force scales is of fundamental research interest.<sup>2–5</sup> The past few decades have witnessed great progress on polymer mechanochemistry, which opens a new avenue for the design of self-reporting polymers with functional mechanophores as stress probes.<sup>6–9</sup> Along the polymer backbones or within the cross-links, these motifs that contain mechanically labile bonds, undergo disruption upon mechanical activation, thereby converting mechanical energy into chemical energy.<sup>10–14</sup> Particularly, mechanochromic or mechanoluminescent polymers, that can generate visualized signals of absorption or fluorescence under applied force, promise the quantitative and locally resolved detection of stress.<sup>15,16</sup> Great efforts have been devoted

to devising new mechanophores with attractive optomechanical properties upon exerting different types and magnitudes of forces.<sup>17–25</sup>

Rhodamine (**Rh**) and bis(adamantyl)-1,2-dioxetane (**Ad**) have been demonstrated as versatile self-reporting mechanophores (Fig. 1a).<sup>17,19</sup> When covalently coupled with polyurethane chains or networks, **Rh** experiences ring-opening transition under stress.<sup>19,26</sup> Discoloration and fluorescence thus arise for high-contrast stress detection, since the ring opened **Rh** exhibits excellent optical properties including a high absorption coefficient and quantum efficiency with long-wavelength absorption and emission. However, exhibiting a more or less persistent mechanochromic response, the non-scissile, reversible **Rh** delivers limited temporal resolution in recording chain scission events.<sup>26,27</sup> In this sense, real-time monitoring of bond breakage is possible when bis(adamantyl)-1,2-dioxetane is integrated as a chemiluminescent stress probe.<sup>17</sup> Mechanical dissociation of the dioxetane ring leads to the excited adamantanone that relaxes to the ground state with blue auto-luminescence (*ca.* 420 nm). Unlike **Rh**, benefiting from the wide dynamic range of chemiluminescence without external excited sources required, **Ad**-derivatized polymers feature high spatial and temporal resolution of mechanochemiluminescence, which results in highly localized emission in front of a propagating crack tip.<sup>28</sup> But due to the low quantum efficiency of the transient blue

Department of Chemistry, Key Laboratory of Mechanism Theory and Equipment Design of State Ministry of Education, Tianjin University, Tianjin, 300354, China. E-mail: yulan.chen@tju.edu.cn

† Electronic supplementary information (ESI) available: General experimental details; RGB analysis; synthetic procedures; GPC curves; NMR spectra; UV-vis spectra; solid-state FL spectra; EM images; DSC curves and supplementary videos. See DOI: 10.1039/d0sc06140a



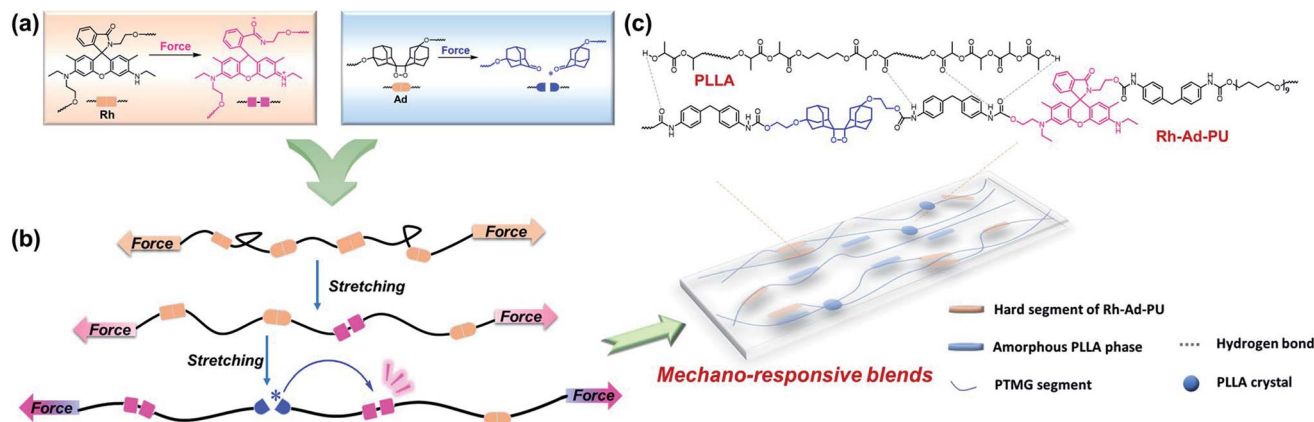


Fig. 1 (a) Chemical structures of bis(adamantyl)-1,2-dioxetane (**Ad**), rhodamine (**Rh**) and their force activated states. (b) Schematic of mechanically induced breakage of **Rh** and **Ad** in a multiblock polymer chain, resulting in mechanochromic and FRET promoted mechanochemiluminescent responses. (c) Chemical structures of PLLA and **Rh-Ad-PU**; several types of hydrogen-bond interactions in blends are illustrated.

emission from broken **Ad**, its mechanical monitoring has to be performed in the dark. Another limitation lies in the high stability of **Ad**, so that its force threshold is fairly high.<sup>29</sup>

Our motivation was to create more sophisticated mechano-responsive polymers to self-report excessive stress with clearly perceptible signals, meanwhile with the rupture force tailored over a broad range. Rather than synthetic elaborations of mechanophores, combining mechanochromic and mechanochemiluminescent moieties is a straightforward and useful approach.<sup>2</sup> Firstly, orthogonal optical properties (absorption and luminescence) can be employed for multimodal analysis of damage and stress. Secondly, the force threshold that triggers discoloration and luminescence or the sensitivity of the rate to the applied force can be adjusted facilely.

Considering the complementary advantages of **Rh** and **Ad**, together with the large difference in their force free potential energies,<sup>26,29</sup> we herein incorporated the two distinct mechanophores into polymer blends of polyurethane and polylactic acid that displayed successive occurrences of mechanochromism and mechanochemiluminescence. The rupture of the **Rh** ring was observed at a low strain, followed by the breakage of **Ad**, concomitant with intense red emission through effective fluorescence resonance energy transfer (FRET) from excited adamantane to the opened zwitterion of **Rh** (Fig. 1b). Notably, although the two mechanophores have been well studied individually, they as well as other chromic mechanophores can only respond under specific loading force either under daylight or in darkness.<sup>30–36</sup> Using this strategy, limitations derived from the large force threshold of **Ad** and limited resolution of **Rh** have been overcome, empowering the polymer blends with abilities to report whether, where and when mechanical events take place, which can work as a full-day stress sensor responsive in an expanded force region.

## Results and discussion

As shown in Fig. 1c, the polymer blends are composed of dual mechano-responsive polyurethane (**Rh-Ad-PU**) as a matrix and

hydroxyl terminated low molecular weight polylactic acid (**PLLA**) as a polymeric filler. With the availability of bis-hydroxyl functionalized **Rh** and **Ad**, **Rh-Ad-PU** containing the two mechanophores (molar ratio = 1 : 1) in the main chain was synthesized through mild polycondensation (synthetic details are described in ESI, Fig. S1, S2 and S5†). Upon fracture, the **Rh-Ad-PU** film changed its color from colorless to red slightly (Fig. S6a†). Meanwhile, if tested in the dark, the film emitted weak red light (Fig. S6b†). Such optical alterations from **Rh-Ad-PU** facilitate its utility as self-reporting stress probe in a complementary manner, that is valid both under daylight and in the dark. The **Rh-Ad-PU** with dual-responsiveness was further explored by integrating it into polymer blends whose mechanical properties and rupture force can be tuned over a broad range. Through this method, the self-reporting performance of the blends is expected to be highlighted, since their broadly tunable mechanical properties would facilitate the mechano-activation of the two mechanophores at distinctly different thresholds.

For that, **PLLA** existing in the forms of crystalline and amorphous phase in blends was selected as a polymeric filler. The chemical and physical features of **PLLA** play an important role in the ultimate performance profile of the multiphase blends: (1) the crystalline domains of **PLLA** with high modulus and their orientation behaviors under applied force can reinforce the blends with increased tensile strength and toughness;<sup>37–39</sup> (2) the amorphous parts facilitate the formation of hydrogen bonds with polyurethane and the ordering of the amorphous phase is responsive and tunable under tension, which are effective in toughening polyurethane.<sup>37,40</sup> Translucent polymer blends **PU/PLLAs** with varied ratios of **PLLA** from 0 to 20 wt% were prepared *via* the solution casting method (details of the preparation are described in ESI, Table S1†). The transparency of the blends decreased with the increase of the crystalline **PLLA** content (Fig. S7†), indicating an increase of phase separation between **PU** and **PLLA**. This result agreed with the morphological observations by transmission electron microscopy. The phase separation of **PU** itself was not very obvious,



with a phase size of only tens of nanometers (Fig. S8a†), which could be ascribed to the weak aggregation of hard segments,<sup>41</sup> whereas all the blends displayed a distinct two-phase morphology with the crystalline phase domains which became significant from **PU/PLLA-5%** to **PU/PLLA-20%** (Fig. S8b–d†). Besides, DSC measurements supported that all the blends were elastomers, as evidenced by their low glass transition temperature ( $T_{g1} < 0$  °C, Fig. S9†). In detail,  $T_g$  associated with the **Rh-Ad-PU**-rich phase first increased (from  $-26$  °C for **PU** to  $-15$  °C for **PU/PLLA-5%**) mainly due to the restricted chain movement by hydrogen bonding between **Rh-Ad-PU** and **PLLA**; then, shifted to a lower temperature ( $-18$  °C for **PU/PLLA-10%**,  $-20$  °C for **PU/PLLA-20%**) with the emergence of the melting peak for **PLLA** at higher **PLLA** content, which could be ascribed to the increase of immiscibility between polyurethane and **PLLA** crystals.<sup>42–44</sup>

The polymer films were then subjected to optomechanical studies on a rheometer equipped with an Expansion Instruments SER Universal Testing Platform, and in connection with a camera to record the discoloration and luminescence information (details in the ESI†). As shown in Fig. 2a, the rupture stress of these blends increased prominently compared with **PU/PLLA-0%**, which was considered to be associated with the reinforced effect of **PLLA**. Among them, **PU/PLLA-10%** with medial size of phase domain exhibited superior mechanical properties. As for **PU/PLLA-20%**, further increasing the **PLLA** loading imposed a negative effect on its mechanical response. This was probably owing to the increased **PLLA** crystalline domains that led to the decrease of compatibility of **PLLA** and polyurethane. Such changes in mechanical properties reflected the importance of the balance between phase separation and crystallinity in these multiphase polymer systems.<sup>44–46</sup> Meanwhile, **PU/PLLAs** are mechanochromic, as can be readily distinguished by the naked eye (Fig. 2b). The ruptured, colored films displayed a characteristic absorption peak (550 nm) of the planar zwitterion from **Rh**; meanwhile, a fluorescence band peaking at 590 nm was detected when the broken film was excited with a 420 nm light source, corresponding to the ring-opening of **Rh** under mechanical force (Fig. S10†).<sup>19</sup> Moreover, since the mechanochromic performance was stress-sensitive, samples with higher rupture stress showed more pronounced discoloration. This finding is essential for **Rh** as a stress sensor in the blends. A more quantitative study of chromism was done by calculating the RGB ratios of the sequential images extracted from the videos (Fig. S11†). The bandpass of the green channel

is well aligned with the absorption band of the zwitterion isomer of **Rh**.<sup>47</sup> Herein, the green channel was used to analyze the extent of discoloration. As for the blends **PU/PLLAs**, the change of the green channel intensity increased along with their tensile stress (Fig. 2b). However, the failure of control specimen **Control-PU/PLLA-10%** (Table S1†) did not present appreciable changes (Fig. S12†). Such comparison also proved that the green channel was related to the generation of red color in a mechanochemical manner.

In darkness, transient intense light from the stretched blends was recorded by using a high-speed camera. The evolution of mechanoluminescence from a representative film demonstrated its high spatial and temporal resolution (Fig. 3). Besides, the light intensity in the 5 ms time span of the fracture frame relative to total light intensity is about 41%, manifesting a high concentration of molecular disruption occurring at the fracture site. In relative to polyurethane containing 1,2-dioxetane as the only mechanophore, the emission color from **PU/PLLAs** varied from blue to red with a remarkable increase in light recognition.<sup>48</sup> This unique mechanoluminescence is attributed to the large difference in stability and mechano-responsive behaviors between the two distinct mechanophores (discussed below).

To gain a better understanding of the mechanochemical transduction from these self-reporting blends, the effects of **PLLA** content and strain rate on the mechanochromism and mechanoluminescence were studied. The total light intensity was found to correlate with mechanical stress. As shown in Fig. 4a, the cumulative intensity from **PU/PLLA-10%** was about 5 times higher than that of **PU/PLLA-0%** (**Rh-Ad-PU** without **PLLA**), despite the diluting effect of inactive **PLLA** in the blends. Compared to the mechanochromic variation (Fig. 2b), the effect of the **PLLA** content on the increment of luminescence was increased, which mainly benefited from the FRET procedure from broken **Ad** to the zwitterion of **Rh**. The boosted intensity strengthens the self-reporting ability of the blends with improved resolution and sensitivity.

Following this, taking **PU/PLLA-10%** for example, the strain-rate-dependent mechanical response was estimated. Fig. 4b shows that decreasing the strain rate from  $5.0$   $s^{-1}$  to  $0.2$   $s^{-1}$  increased the mechanical properties dramatically in terms of

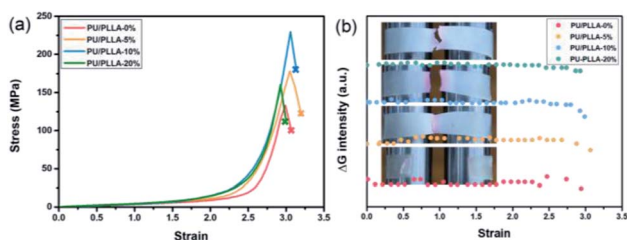


Fig. 2 (a) Stress–strain curves and (b) the changes in the green channel upon straining different films at a strain rate of  $1.0$   $s^{-1}$ ; insets show the fracture of polymer films.

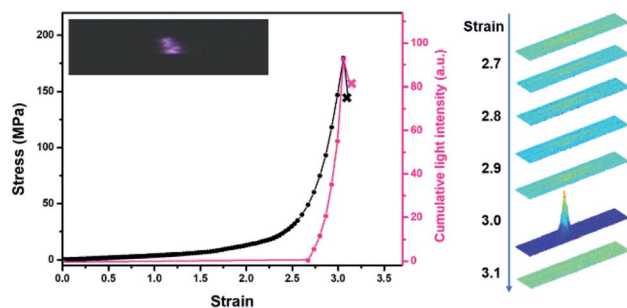


Fig. 3 Stress and cumulative light intensity vs. strain during stretching of the **PU/PLLA-10%** film at a strain rate of  $1.0$   $s^{-1}$ . The right graph corresponds to intensity analysis of the stretched sample. The analysed intensity is based on the same region within the sample.



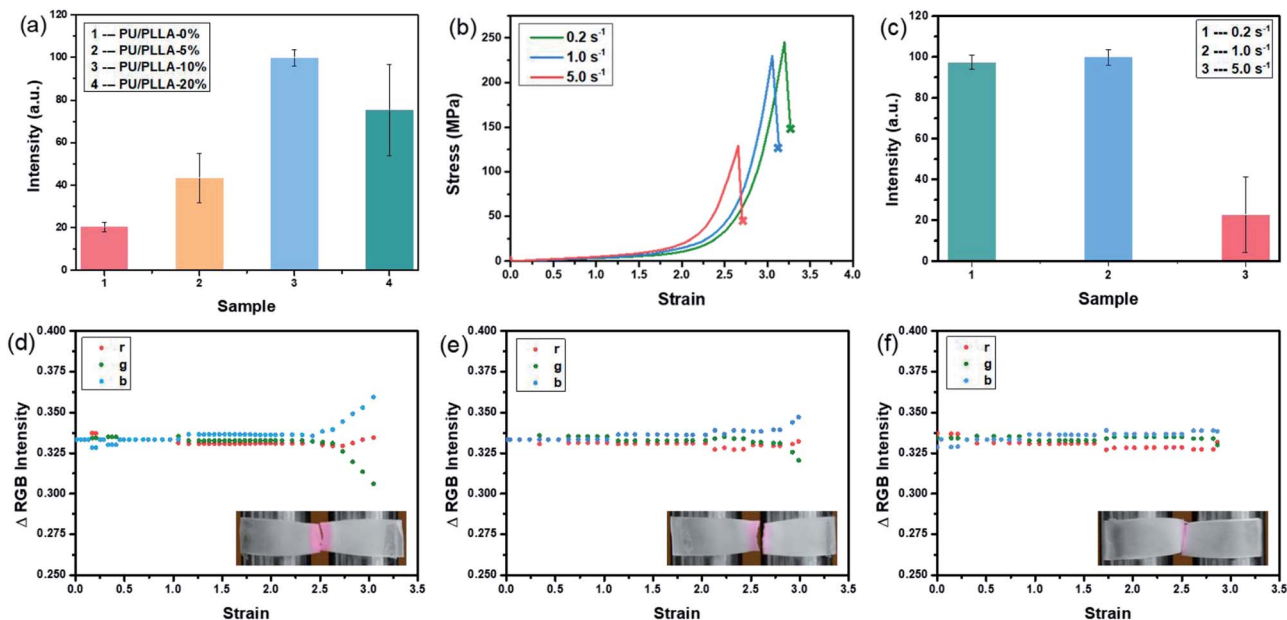


Fig. 4 (a) Total light intensity emitted upon stretching PU/PLLA films at a strain rate of  $1.0 \text{ s}^{-1}$ . (b) Stress–strain curves; (c) total light intensity emitted upon stretching films of PU/PLLA-10% at different strain rates. Relative change in RGB intensity upon stretching films of PU/PLLA-10% at a strain rate of (d)  $0.2 \text{ s}^{-1}$ ; (e)  $1.0 \text{ s}^{-1}$ ; (f)  $5.0 \text{ s}^{-1}$ ; insets show the fracture of PU/PLLA-10% films.

strength and toughness. Also, the slower strain rate on the sample led to a more significant color change and luminescence intensity (Fig. 4c–f, Video S1 and S2†). Since the intensity of red light was proportional to the number of activated mechanophores, these results supported that, at a lower strain rate, mechanochemical transduction was more efficient, so that more **Rh** and **Ad** were activated in our blends. Generally, for most non-microphase-separated polymers, chain disentanglement is slowed down effectively at high tension rates, leading to more efficient mechanochemical transition.<sup>49</sup> In our study, such discrepancy with respect to the negative strain-rate related mechanical responsive behaviors might arise from other unique interactions. The disassociation of numerous hydrogen bonds can remarkably consume the strain energy, and contributes to the significant improvement of toughness.<sup>50</sup> Besides, strain-induced orientation is a well-known characteristic of PLLA reinforced elastomers.<sup>37,38,40</sup> The two factors are kinetically controllable, which is favored under low strain rate, but negligible for ameliorating mechanical properties as well as for bond scission events at high rates.<sup>51</sup> As shown in Fig. S13,† after slow stretching, the film orientation lying parallel to the tensile axis was observed.

Notably, although **Ad** in the force free state seems much more stable than **Rh** ( $E_a$ :  $154.9 \text{ kJ mol}^{-1}$  vs.  $96.2 \text{ kJ mol}^{-1}$ ),<sup>26,29</sup> their chemical conversion under tension is unpredictable. Revealing the competitive mechanochemical process of **Ad** and **Rh** is difficult in theory. This is because the mechanochemiluminescence of dioxetane follows the non-adiabatic dissociation mechanism that largely precludes the well-used quantum-chemical calculations of force-dependent kinetics.<sup>27</sup> Pleasingly, herein experimentally, we found the successful FRET process under tension (Fig. S10†), which in turn indicated a very

likely, successive bond scission process from the two mechanophores. That is, **Rh** units are more labile; part of them are mechanically activated ahead of the breakage of **Ad**, and serve as the fluorescent acceptor of the excited ketone to emit bright red light.

When different mechanophores were coupled closely, a reduction in their mechano-activation was very likely anticipated since they shared the overall stress at separate sites.<sup>10,13,52</sup> To elaborate on this point, reference polymer blends containing **Rh** or **Ad** only (**Rh-PU/PLLA-10%** and **Ad-PU/PLLA-10%**) were prepared for optomechanical studies (Table S1, Fig. S1, S3 and S4†). As shown in Fig. S14,† the discoloration of **Rh-PU/PLLA-10%** and luminescence of **Ad-PU/PLLA-10%** set on at the deformation of *ca.* 278% (*ca.* 79 MPa) and *ca.* 357% (*ca.* 214 MPa), respectively. On the other hand, Fig. 5b and c shows the functions of chromism and light intensity vs. strain for **PU/PLLA-10%** (Video S1 and S2†). As for the bis-mechanophore counterpart, the chromism appeared at a strain of *ca.* 260% (*ca.* 80 MPa); further elongation until a strain of *ca.* 310% (*ca.* 180 MPa) triggered the activation of **Ad**. Valuable information deduced from these data is as follows: (1) a distinct difference in the mechanical activation between **Rh-PU/PLLA-10%** and **Ad-PU/PLLA-10%** was indeed observed, which supported that many of the **Rh** units could be mechanically activated before **Ad**. (2) The existence of an overlapping stress region for chromism and luminescence implicated the simultaneous breakage of a fraction of the two mechanophores after many of the **Rh** rings were opened under low stress. (3) The force thresholds for the respective activation of **Rh-PU/PLLA-10%** and **Ad-PU/PLLA-10%** were similar to those of **PU/PLLA-10%**, except for the slight “shifting” of the chemiluminescent transition to the lower strain in our bis-mechanophore system mainly due to the



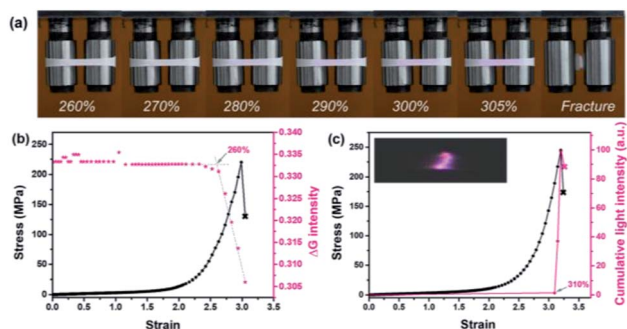


Fig. 5 (a) Pictures illustrating mechanochromism under deformation. (b) Stress and the intensity in the green channel as a function of strain. (c) Stress and cumulative light intensity as a function of strain according to the analysis of representative mechanochromic and mechanoluminescent videos (the PU/PLLA-10% film was stretched at a strain rate of  $0.2 \text{ s}^{-1}$ ).

additional FRET process to sensitize the luminescence signal. Therefore, our results indicated that the difference between **Rh** and **Ad** didn't translate into an observable impact on the activation of **PU/PLLA-10%** in the bulk state, or the mechanochemical coupling effect on the scission rate of adjacent **Rh** and **Ad** was not sufficient enough to be detected.<sup>52</sup>

Additionally, through this coupling method, not only a versatile analysis of material damage can be realized *via* two different manifestations, but also the stress history can be captured, in that the distinctive change of chemiluminescence color from blue to red recorded a prior force-loading on the **Rh** moieties (Fig. 5a). Importantly, since the two specific bond rupture events can be stimulated at highly different mechanical levels, expanding the responsive force range from these mechano-sensing blends now can be realized. Overall, the limitation arising from the high stability of the mechanochemiluminescent polymers with **Ad** alone now can be overcome, with effectively "shifting" the appreciable optical changes to a much lower force threshold, and meanwhile exhibiting a more dynamic change upon the deformation process. This finding is highly helpful for probing the stress evolution of the damaged samples over a broader force range with high resolution that was not able to be addressed previously.

## Conclusion

We have developed a new class of stress-reporting **PU/PLLA** blends by merging dual distinct mechanochromic and mechanochemiluminescent units (**Rh** and **Ad**) into polymer main chains. The two mechanophores can be activated and exhibit red discoloration and red chemiluminescence, respectively, according to the different strengths of mechanical stimuli. Taking advantage of the two mechanophores, the yielded macroscopically detectable optical signals from these blends have been proved as stress-dependent, with high resolution to report the evolution and localization of damage at the molecular scale, which cannot be realized by using one mechanophore alone. Furthermore, the fact that mechanically generated

discoloration takes place obviously earlier than that of luminescence, not only indicates an expanded responsive force range, but also in turn, confirms that the activation energy of **Rh** is less than that of **Ad** under mechanical conditions. Our strategy thus is applicable for the comparison of the bond energy of different mechanophores, even if it is difficult theoretically. Also, setting aside the enormous synthetic efforts on new multi-functional mechanophores, the present approach is versatile in unravelling and enhancing mechanochemical processes at the molecular level; thus, it can facilitate the full-day stress detection in a multimodal analysis.

## Conflicts of interest

There are no conflicts to declare.

## Acknowledgements

Financial support by the National Key Research and Development Program of China (Grants 2017YFA0204503 and 2017YFA0207800) and the National Natural Science Foundation of China (Grants 21975178 and 21734006) is acknowledged.

## Notes and references

- M. M. Caruso, D. A. Davis, Q. Shen, S. A. Odom, N. R. Sottos, S. R. White and J. S. Moore, *Chem. Rev.*, 2009, **109**, 5755–5798.
- T. Kosuge, X. Zhu, V. M. Lau, D. Aoki, T. J. Martinez, J. S. Moore and H. Otsuka, *J. Am. Chem. Soc.*, 2019, **141**, 1898–1902.
- J. Wang, T. B. Kouznetsova, R. Boulatov and S. L. Craig, *Nat. Commun.*, 2016, **7**, 13433.
- Y. Sha, Y. Zhang, E. Xu, W. McAlister, T. Zhu, S. L. Craig and C. Tang, *Chem. Sci.*, 2019, **10**, 4959–4965.
- B. H. Bowser and S. L. Craig, *Polym. Chem.*, 2018, **9**, 3583–3593.
- J. R. Arino and D. Marx, *Chem. Rev.*, 2012, **112**, 5412–5487.
- L. Takacs, *Chem. Soc. Rev.*, 2013, **42**, 7649–7659.
- C. L. Brown and S. L. Craig, *Chem. Sci.*, 2015, **6**, 2158–2165.
- T. Stauch and A. Dreuw, *Chem. Rev.*, 2016, **116**, 14137–14180.
- B. Lee, Z. Niu, J. Wang, C. Sledobnick and S. L. Craig, *J. Am. Chem. Soc.*, 2015, **137**, 10826–10832.
- M. K. Beyer and H. Clausen-Schaumann, *Chem. Rev.*, 2005, **105**, 2921–2948.
- G. De Bo, *Chem. Sci.*, 2018, **9**, 15–21.
- M. Zhang and G. De Bo, *J. Am. Chem. Soc.*, 2020, **142**, 5029–5033.
- D. Yildiz, C. Baumann, A. Mikosch, A. J. C. Kuehne, A. Herrmann and R. Göstl, *Angew. Chem., Int. Ed.*, 2019, **58**, 12919–12923.
- C. Calvino, L. Neumann, C. Weder and S. Schrettl, *J. Polym. Sci., Part A: Polym. Chem.*, 2017, **55**, 640–652.
- Y. Yuan and Y. Chen, *Chin. J. Polym. Sci.*, 2017, **35**, 1315–1327.



- 17 Y. Chen, A. J. H. Spiering, S. Karthikeyan, G. W. M. Peters, E. W. Meijer and R. P. Sijbesma, *Nat. Chem.*, 2012, **4**, 559–562.
- 18 K. Imato, A. Irie, T. Kosuge, T. Ohishi, M. Nishihara, A. Takahara and H. Otsuka, *Angew. Chem., Int. Ed.*, 2015, **54**, 6168–6172.
- 19 Z. Wang, Z. Ma, Y. Wang, Z. Xu, Y. Luo, Y. Wei and X. Jia, *Adv. Mater.*, 2015, **27**, 6469–6474.
- 20 A. Lavrenova, D. W. R. Balkenende, Y. Sagara, S. Schrettl, Y. C. Simon and C. Weder, *J. Am. Chem. Soc.*, 2017, **139**, 4302–4305.
- 21 Y. Sagara, M. Karman, E. Verde-Sesto, K. Matsuo, Y. Kim, N. Tamaoki and C. Weder, *J. Am. Chem. Soc.*, 2018, **140**, 1584–1587.
- 22 M. D. Giannantonio, M. A. Ayer, E. Verde-Sesto, M. Lattuada, C. Weder and K. M. Fromm, *Angew. Chem., Int. Ed.*, 2018, **57**, 11445–11450.
- 23 H. Zhang, D. Zeng, Y. Pan, Y. Chen, Y. Ruan, Y. Xu, R. Boulatov, C. Creton and W. Weng, *Chem. Sci.*, 2019, **10**, 8367–8373.
- 24 M. E. McFadden and M. J. Robb, *J. Am. Chem. Soc.*, 2019, **141**, 11388–11392.
- 25 Y. Lin, T. B. Kouznetsova and S. L. Craig, *J. Am. Chem. Soc.*, 2020, **142**, 99–103.
- 26 T. Wang, N. Zhang, J. Dai, Z. Li, W. Bai and R. Bai, *ACS Appl. Mater. Interfaces*, 2017, **9**, 11874–11881.
- 27 S. Akbulatov and R. Boulatov, *ChemPhysChem*, 2017, **18**, 1422–1450.
- 28 E. Ducrot, Y. Chen, M. Bulters, R. P. Sijbesma and C. Creton, *Science*, 2014, **344**, 186–189.
- 29 G. B. Schuster, N. J. Turro, H.-C. Steinmetzer, A. P. Schaap, G. Paler, W. Adam and J. C. Liu, *J. Am. Chem. Soc.*, 1975, **97**, 7110–7118.
- 30 L. Wang, K. Yang, Q. Zhou, H. Yang, J. He and X. Zhang, *Chin. J. Polym. Sci.*, 2020, **38**, 24–36.
- 31 L. Wang, W. Zhou, Q. Tang, H. Yang, Q. Zhou and X. Zhang, *Polymers*, 2018, **10**, 994.
- 32 G. Kim, V. M. Lau, A. J. Halmes, M. L. Oelze, J. S. Moore and K. C. Li, *Proc. Natl. Acad. Sci. U.S.A.*, 2019, **116**, 10214–10222.
- 33 Z. S. Kean, J. L. Hawk, S. Lin, X. Zhao, R. P. Sijbesma and S. L. Craig, *Adv. Mater.*, 2014, **26**, 6013–6018.
- 34 Y. Yuan, W. Chen, Z. Ma, Y. Deng, Y. Chen and W. Hu, *Chem. Sci.*, 2019, **10**, 2206–2211.
- 35 J. M. Clough and R. P. Sijbesma, *ChemPhysChem*, 2014, **15**, 3565–3571.
- 36 J. M. Clough, A. Balan, T. L. J. van Daal and R. P. Sijbesma, *Angew. Chem., Int. Ed.*, 2016, **55**, 1445–1449.
- 37 L. Shi, R.-Y. Zhang, W.-B. Ying, H. Hu, Y.-B. Wang, Y.-Q. Guo, W.-Q. Wang, Z.-B. Tang and J. Zhu, *Chin. J. Polym. Sci.*, 2019, **37**, 1152–1161.
- 38 V. Jašo, M. V. Rodićb and Z. S. Petrovic, *Eur. Polym. J.*, 2015, **63**, 20–28.
- 39 H. Sun, J. Hu, X. Bai, Z. Zheng, Z. Feng, N. Ning, L. Zhang and M. Tian, *Polym. Test.*, 2017, **64**, 250–253.
- 40 W. Lin and J.-P. Qu, *Ind. Eng. Chem. Res.*, 2019, **58**, 10894–10907.
- 41 Y. He, J. Zeng, G. Liu, Q. Li and Y. Wang, *RSC Adv.*, 2014, **4**, 12857–12866.
- 42 P. Song, Z. Xu and Q. Guo, *ACS Macro Lett.*, 2013, **2**, 1100–1104.
- 43 S. Liu, Y. Yuan, J. Li, S. Sun and Y. Chen, *Polym. Chem.*, 2020, **11**, 1877–1884.
- 44 C.-W. A. Ng, M. J. Lindway and W. J. MacKnight, *Macromolecules*, 1994, **27**, 3027–3032.
- 45 X. Hu, Y. Li, M. Li, H. Kang and L. Zhang, *Ind. Eng. Chem. Res.*, 2016, **55**, 9195–9204.
- 46 B. K. Sharma, A. Stoesser, S. K. Mondal, S. K. Garlapati, M. H. Fawey, V. S. K. Chakravadhanula, R. Kruk, H. Hahn and S. Dasgupta, *ACS Appl. Mater. Interfaces*, 2018, **10**, 22408–22418.
- 47 D. A. Davis, A. Hamilton, J. Yang, L. D. Cremer, D. V. Gough, S. L. Potisek, M. T. Ong, P. V. Braun, T. J. Martinez, S. R. White, J. S. Moore and N. R. Sottos, *Nature*, 2009, **459**, 68–72.
- 48 F. Yang, Y. Yuan, R. P. Sijbesma and Y. Chen, *Macromolecules*, 2020, **53**, 905–912.
- 49 Y. Chen and R. P. Sijbesma, *Macromolecules*, 2014, **47**, 3797–3805.
- 50 Y. Chen, H. Zhang, X. Fang, Y. Lin, Y. Xu and W. Weng, *ACS Macro Lett.*, 2014, **3**, 141–145.
- 51 R. Lv, B. Na, N. Tian, S. Zou, Z. Li and S. Jiang, *Polymer*, 2011, **52**, 4979–4984.
- 52 R. Stevenson, M. Zhang and G. De Bo, *Polym. Chem.*, 2020, **11**, 2864–2868.

